

Energy-efficient Stochastic Connected Cruise Control

Minghao Shen¹, Chaozhe R. He^{1,2}, A. Harvey Bell¹, and Gábor Orosz^{1,3}

Abstract—An energy-efficient longitudinal controller is designed for connected automated trucks traveling in mixed traffic environment, consisting of connected and non-connected vehicles. A data-driven optimization method is proposed to determine the parameters of the energy-optimal controller while modeling the speed of nearby vehicles as stochastic processes. Spectral estimation is utilized for the analysis of the linearized system and the efficacy of our proposed method is evaluated statistically using synthetic data.

I. INTRODUCTION

Improving the energy efficiency of heavy duty vehicles can bring great environmental and financial benefits for freight transportation. Previous research has shown that applying different longitudinal controllers may result in significant differences in energy consumption [1]. Thus, an effective way of improving energy efficiency is to optimize the longitudinal control design. This may bring benefits to trucks with different powertrains (internal combustion engines, battery electric and hybrid electric).

Adaptive cruise control(ACC) is a popular longitudinal controller, which determines the acceleration of host vehicle utilizing the measurement of position and speed of vehicle immediately in the front. Wireless vehicle-to-everything (V2X) communication may bring new opportunities in improving energy efficiency. When a group of connected automated vehicles are following each other closely, one may utilize cooperative adaptive cruise control (CACC) algorithms in order to save energy [2], [3], [4], [5]. However, the penetration of connected and automated vehicles is still very low, demanding strategies that may enable energy savings for lean penetration of connectivity and automation. Connected cruise control (CCC) exploits information from V2X connectivity with the reachable connected vehicles in traffic [6], [7], and this may lead to significant energy savings [8].

One of the main challenges is that vehicles ahead may exhibit a large variety of different motions and a controller that ensures high energy efficiency for one profile may perform poorly for another one. V2X connectivity allows vehicles to obtain information from beyond line of sight [9], making it possible to make better predictions in traffic [10], [11], [12]. One can optimize the longitudinal controller based on the prediction of motions of preceding vehicles [13], [14],

but this heavily relies on the accuracy of prediction. While long prediction horizon is needed to save energy [8], the uncertainty of prediction grows rapidly with the prediction horizon. In this paper, instead of pursuing more precise prediction of transient human behavior, we optimize the energy consumption in the average sense for stationary motion. In particular, we propose a stochastic modeling framework for the vehicles' motion and apply spectral methods to evaluate the effects of controller. The spectral properties of vehicle motion are estimated using data collected via V2X. Therefore our method is non-parametric and requires no first-principle driver models. The controller parameters are optimized according to traffic data and the optimality of the controller parameters are validated statistically with large amount of synthetic data.

This rest of the paper is organized as follows. Section II describes the problem setting and proposes a longitudinal controller that utilizes information obtained via V2X communication. Section III describes the stochastic modeling of vehicle trajectories. Section IV proposes a method to determine the control parameters that minimize the average energy consumption. Section V evaluates the energy efficiency for adaptive cruise control and connected cruise control. Section VI summarizes the results and lay out future research directions..

II. CONNECTED CRUISE CONTROL DESIGN

In this section, we design a longitudinal controller for connected automated truck (CAT) traveling in a mixed traffic consisting of connected human-driven vehicles (CHVs) and non-connected human-driven vehicles (HVs) shown in Fig. 1(a). We assume that the truck senses the vehicle immediately ahead using range sensors (e.g., radar or LIDAR) and can also communicate with another preceding vehicle ahead via vehicle-to-vehicle (V2V) communication. The longitudinal controller of the CAT shall respond to the motion of all vehicles from which it obtains information (either by sensors or via V2V communication. We refer to this concept as connected cruise control (CCC) which has been investigated both theoretically [6], [7] and experimentally [15]. Here we focus on the energy benefits of this strategy following the concepts laid out in [8].

We model the longitudinal dynamics of the truck using the differential equations

$$\begin{aligned} \dot{h}(t) &= v_1(t) - v(t), \\ \dot{v}(t) &= -f(v(t)) + \text{sat}(u(t - \sigma)), \end{aligned} \quad (1)$$

where v and v_1 denote the speed of the truck and the vehicle right in the front of it, while h is the distance headway be-

This work was supported by Navistar, Inc.

¹M. Shen, C. R. He, A. H. Bell, and G. Orosz are with the Department of Mechanical Engineering, University of Michigan, Ann Arbor, MI 48109, USA {mhshen, hchaozhe, ahbelliv, orosz}@umich.edu

²C. R. He is also with Navistar, Inc. Lisle, IL 60532, USA Chaozhe.He@navistar.com

³G. Orosz is also with the Department of Civil and Environmental Engineering, University of Michigan, Ann Arbor, MI 48109, USA

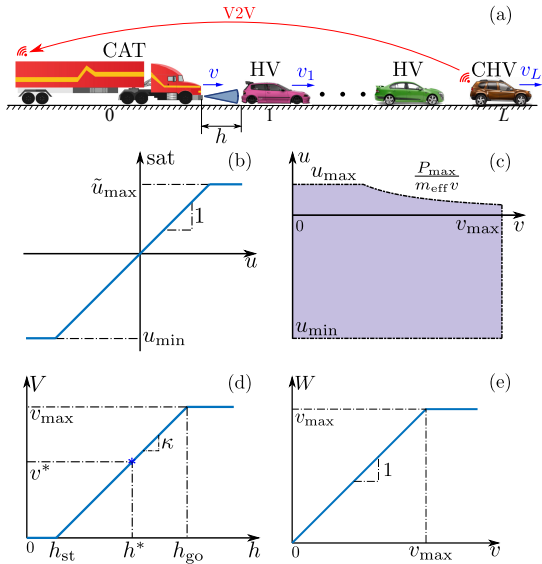


Fig. 1. (a) A connected automated truck (CAT) driving in a mixed traffic consisting of connected human-driven vehicles (CHVs) and non-connected human-driven vehicles (HVs). (b,c) Saturation function (2) (3). (d) Range policy (6). (e) Speed policy (14).

tween them. The resistance term $f(v) = c_0 + c_1 v^2$ originate from the rolling resistance and the air drag and we neglect the road grade for simplicity. Here we use $c_0 = 0.0585$ [m/s²] and $c_1 = 1.30 \times 10^{-4}$ [1/m] adopted from [8].

The effect of control input u appear in (1) after some time delay and it is subject to saturation. The time delay σ models the delay in the powertrain system while saturation results from the limited available braking torque, engine torque, and engine power. In particular we have

$$\text{sat}(u) = \max \{u_{\min}, \min\{u, \tilde{u}_{\max}\}\} \quad (2)$$

where

$$\tilde{u}_{\max} = \min \left\{ u_{\max}, \frac{P_{\max}}{m_{\text{eff}} v} \right\}, \quad (3)$$

that are visualized in Fig. 1(b,c). Here we consider the parameters $u_{\min} = -4$ [m/s²], $u_{\max} = 1$ [m/s²], $P_{\max} = 300.65$ [kW], $m_{\text{eff}} = 29641$ [kg]; see [8].

In this paper we propose the controller

$$u(t) = \tilde{f}(v(t)) + a_d(t), \quad (4)$$

where compensation term $\tilde{f}(v(t))$ is implemented by the lower level controller in order to cancel the resistance term, while a_d defines the desired acceleration given by the higher level controller. We use \mathcal{I} to denote the set of vehicles whose motion information the CAT has access to. This includes vehicle 1 which is monitored by the range sensors, as well as the CHVs who share their motion information via V2X connectivity. Here we consider controllers of the form

$$a_d = \alpha(V(h) - v) + \sum_{i \in \mathcal{I}} \beta_i (W(v_i) - v), \quad (5)$$

where the first term is designed to maintain the headway and the second term aims to match the speed with the speed of the preceding vehicles.

The controller (5) contains the range policy

$$V(h) = \max \{0, \min\{\kappa(h - h_{\text{st}}), v_{\max}\}\}, \quad (6)$$

depicted in Fig. 1(d). For small headway the truck tends to stop, for large headway it aims to travel with maximum speed v_{\max} , while between the desired speed increases linearly with gradient $\kappa = v_{\max}/(h_{\text{go}} - h_{\text{st}})$. In addition, the speed policy

$$W(v) = \min\{v, v_{\max}\}, \quad (7)$$

shown Fig. 1(e) is designed to keep the speed below the limit v_{\max} in case the preceding vehicles are speeding. In this paper we set $v_{\max} = 35$ [m/s], $h_{\text{st}} = 5$ [m], $h_{\text{go}} = 55$ [m], yielding $\kappa = 0.6$ [1/s].

In order to study the performance of the controller we linearize the closed loop system (1,4,5) about the equilibrium

$$h(t) \equiv h^*, \quad v(t) = v_i(t) \equiv v^* = V(h^*), \quad (8)$$

for $i \in \mathcal{I}$. Defining headway and speed perturbations $\tilde{h} = h - h^*$, $\tilde{v} = v - v^*$, $\tilde{v}_i = v_i - v^*$ we obtain

$$\begin{aligned} \dot{\tilde{h}}(t) &= \tilde{v}_1(t) - \tilde{v}(t), \\ \dot{\tilde{v}}(t) &= \alpha(\kappa \tilde{h}(t - \sigma) - \tilde{v}(t - \sigma)) \\ &\quad + \sum_{i \in \mathcal{I}} \beta_i (\tilde{v}_i(t - \sigma) - \tilde{v}(t - \sigma)). \end{aligned} \quad (9)$$

Applying the Laplace transform with zero initial condition leads to

$$V(s) = \sum_{i \in \mathcal{I}} T_i(s) V_i(s), \quad (10)$$

where $V(s)$ and $V_i(s)$ denote the Laplace transform of the speed of the CAT $v(t)$ and the speed of the preceding vehicles $v_i(t)$, while the so-called link transfer functions are defined as

$$T_1(s) = \frac{\beta_1 s + \alpha \kappa}{\mathcal{D}(s)}, \quad T_i(s) = \frac{\beta_i s}{\mathcal{D}(s)}, \quad (11)$$

for $i \in \mathcal{I} \setminus \{1\}$ where

$$\mathcal{D}(s) = s^2 e^{s\sigma} + \left(\alpha + \sum_{i \in \mathcal{I}} \beta_i \right) s + \alpha \kappa. \quad (12)$$

In order to ensure that the truck is able to approach the equilibrium (8), the linearized system (9) needs to be plant stable [6]. That is, all roots of the characteristic equation $\mathcal{D}(s) = 0$ must have negative real parts. This is satisfied if the parameters $(\alpha, \beta_i), i \in \mathcal{I}$ are selected from the region Ω :

$$\begin{aligned} \alpha &> 0, \\ \underline{\omega} \sin(\underline{\omega}\sigma) - \alpha &\leq \sum_{i \in \mathcal{I}} \beta_i < \bar{\omega} \sin(\bar{\omega}\sigma) - \alpha, \end{aligned} \quad (13)$$

where $\underline{\omega}$ and $\bar{\omega}$ are the solutions of transcendental equation $\alpha \kappa = \omega^2 \cos(\omega\sigma)$ such that $0 < \underline{\omega} < \bar{\omega} < \frac{\pi}{2}$.

To evaluate the energy consumption of the CAT, we use energy consumption per unit mass in time interval $t \in [t_0, t_f]$:

$$w = \int_{t_0}^{t_f} v(t) g(\dot{v}(t) + f(v(t))) dt, \quad (14)$$

where $g(x) = \max\{x, 0\}$. Our goal is to find the combinations of the control gains $(\alpha, \beta_i), i \in \mathcal{I}$ that minimize w while also ensuring plant stability.

III. STOCHASTIC MODELING

In this section, we propose a stochastic approach where we model the motion of the preceding vehicles using stochastic processes. For simplicity, we limit our analysis on a specific family of stochastic processes, called Gaussian processes, which result in physically realistic vehicle motions.

Consider a closed loop system with dynamics (1,4,5) where the inputs $v_i, i \in \mathcal{I}$ are stochastic processes. The goal is to relate the gain parameters $(\alpha, \beta_i), i \in \mathcal{I}$ to the system output v and in turn to the energy consumption w defined in (14). To simplify the analysis, we make three assumptions about the input processes $v_i, i \in \mathcal{I}$: (i) They are wide-sense stationary (WSS); (ii) They are differentiable; (iii) They are Gaussian processes. We discuss these assumptions more rigorously below and relate them to spectral theory.

The stationarity assumption enables us to apply spectral analysis, and link the controller parameters to characteristics of output process v . We begin with some definitions.

Definition 1 (Strict-sense Stationary (SSS)). A stochastic process $\{X_t\}_{t \in T}$ is *strict-sense stationary* if for any indices $t_1, \dots, t_k \in T$ and sets A_1, \dots, A_k , the probabilities $\mathbb{P}(X_{t_1+t} \in A_1, \dots, X_{t_k+t} \in A_k)$ do not depend on $t \in T$.

In many cases, strict-sense stationarity can be restrictive. Instead we utilize wide-sense stationary which enforces stationarity on first and second order moments.

Definition 2 (Mean and Correlations). For a stochastic process $\{X_t\}_{t \in T}$, the *mean* and the *autocorrelation* are given by

$$\mu_X(t) = \mathbb{E}[X_t], \quad R_{XX}(s, t) = \mathbb{E}[X_s X_t], \quad (15)$$

where $\mathbb{E}[\cdot]$ denotes the expected value. Considering another stochastic process $\{Y_t\}_{t \in T}$ defined on the same probability space, we define the *cross-correlation*

$$R_{XY}(s, t) = \mathbb{E}[X_s Y_t]. \quad (16)$$

Definition 3 (Wide-sense Stationary (WSS)). A stochastic process $\{X_t\}_{t \in T}$ is called wide-sense stationary if there exist a constant m and a function $r(t)$, $t \in T$, such that

$$\mu_X(t) \equiv m, \quad R_{XX}(s, t) = r(t - s), \quad \forall s, t \in T. \quad (17)$$

When $\{X_t\}_{t \in T}$ is WSS, $R_{XX}(s, t)$ is a function of $(t - s)$ and we write $R_{XX}(\tau) = R_{XX}(t - s)$ without ambiguity. One may verify that autocorrelation is symmetric, that is, $R_{XX}(s, t) = R_{XX}(t, s)$ for a general stochastic process, yielding $R_{XX}(\tau) = R_{XX}(-\tau)$ for a WSS process. Similarly the cross-correlation is also symmetric. Also note that the autocorrelation $R_{XX}(0)$ gives the second moment; cf. (15). We assume that speed perturbations of the preceding vehicles \tilde{v}_i are WSS, that is, $v_i = v^* + \tilde{v}_i$ where v^* denotes the equilibrium speed and $\mu_{\tilde{v}_i} = 0$, for all $i \in \mathcal{I}$.

One major benefit from the WSS assumption is that, we can apply spectral analysis, and thus, determine the input/output relationship for linear time-invariant (LTI) systems. First we define *power spectral density* as the Fourier

transform of autocorrelation function:

$$S_{XX}(\omega) = \mathcal{F}[R_{XX}(\tau)] = \int_{-\infty}^{\infty} R_{XX}(\tau) e^{-j\omega\tau} d\tau, \quad (18)$$

where ω denotes the angular frequency. Since $R_{XX}(\tau) = R_{XX}(-\tau)$, the power spectral density $S_{XX}(\omega)$ is a non-negative real number and one can also show that $S_{XX}(\omega) = S_{XX}(-\omega)$. For LTI systems with input being a WSS process, the power spectral density of the output process can be calculated using the following theorem [16].

Theorem 1 (Spectral Analysis of LTI Systems). For a linear system with transfer function $G(s)$, if the input signal X_t is a WSS process, then the output signal Y_t is also WSS. The first and second order moment of Y_t are given by

$$\mu_Y = G(0)\mu_X, \quad S_{YY}(\omega) = |G(j\omega)|^2 S_{XX}(\omega). \quad (19)$$

Similarly, the *cross power spectral density* can be defined as the Fourier transform of crosscorrelation function

$$S_{XY}(\omega) = \mathcal{F}[R_{XY}(\tau)], \quad (20)$$

which may be a complex number. The following theorem defines the input/output relationship of signal passing through different LTI systems [16].

Theorem 2. Given two signals X_t and Y_t separately passing through two LTI systems with transfer functions $G_1(s)$ and $G_2(s)$, respectively, the cross power spectral density of the corresponding outputs Z_t and Ξ_t is

$$S_{Z\Xi}(\omega) = G_1(j\omega)G_2^*(j\omega)S_{XY}(\omega), \quad (21)$$

where the star denotes the complex conjugate.

Due to physics, the speed of preceding vehicles are continuous and differentiable. The derivative of stochastic processes are often considered in mean square sense; see [16] for details. Specifically, for a WSS process X_t , we have the following properties of the time derivative \dot{X}_t :

- (a) X_t and \dot{X}_t are jointly WSS,
- (b) $\mu_{\dot{X}}(t) = 0$,
- (c) $R_{\dot{X}\dot{X}}(\tau) = \frac{d}{d\tau} R_{XX}(\tau) = -R_{XX}(\tau)$,
- (d) $R_{\dot{X}\dot{X}}(0) = R_{X\dot{X}}(0) = 0$,
- (e) $R_{\dot{X}\dot{X}} = -\frac{d^2}{d\tau^2} R_{XX}(\tau)$.

Apart from being differentiable, the speed of preceding vehicles are assumed to be Gaussian processes. This simplifies the analysis and enables us to derive analytical results.

Definition 4 (Gaussian Process (GP)). A stochastic process $\{X_t\}_{t \in T}$ is a *Gaussian process* if for every finite set of indices $t_1, \dots, t_k \in T$, $X(t_1, \dots, t_k) = (X_{t_1}, \dots, X_{t_k})$ is multivariate Gaussian random variable.

Gaussian process has the following nice properties [16].

- (a) Gaussian process is uniquely determined by its mean function and autocorrelation function.
- (b) If a Gaussian process is WSS, then it is SSS.
- (c) For a linear system, if the input signal is a Gaussian process, then the output is also a Gaussian process.
- (d) If a Gaussian process X_t is mean square differentiable, then \dot{X}_t is also a Gaussian process.

IV. DATA-DRIVEN CONTROLLER OPTIMIZATION

In this section, we propose a method to determine the energy-optimal parameters for the proposed controller using traffic data. First we derive an optimization problem assuming the oracle knowledge of spectral density of preceding vehicles' speed. Then we introduce two estimators for the cross power spectral density, and finally formalize the data-driven controller optimization method.

A. Optimization with oracle knowledge

Here we utilize the concepts introduced in the previous section. We apply spectral analysis for the linearized system (9), derive analytical expression for the expectation of energy consumption defined in (14), and formulate the optimization problem to determine energy-optimal controller parameters.

The inputs \tilde{v}_i , $i \in \mathcal{I}$ are assumed to be WSS, mean-square differentiable Gaussian processes with zero mean. Then the output \tilde{v} is also a WSS Gaussian process with zero mean. According to (10), the output signal \tilde{v} can be decomposed into response to each input signal \tilde{v}_i :

$$\tilde{v}(t) = \sum_{i \in \mathcal{I}} \eta_i(t), \quad (22)$$

According to Theorems 1 and 2, for all $i, j \in \mathcal{I}$ we have

$$\mu_{\eta_i} = 0, \quad S_{\eta_i \eta_j}(\omega) = T_i(j\omega)T_j^*(j\omega)S_{\tilde{v}_i \tilde{v}_j}(\omega), \quad (23)$$

such that when $i = j$

$$S_{\eta_i \eta_i}(\omega) = |T_i(j\omega)|^2 S_{\tilde{v}_i \tilde{v}_i}(\omega). \quad (24)$$

Then taking inverse Fourier transform we calculate the autocorrelations $R_{\eta_i \eta_j}(\tau) = \mathcal{F}^{-1}[S_{\eta_i \eta_j}(\omega)]$ for all $i, j \in \mathcal{I}$, which allow us to calculate the autocorrelation of the speed perturbation \tilde{v} :

$$\begin{aligned} R_{\tilde{v} \tilde{v}}(\tau) &= \mathbb{E}[\tilde{v}(t)\tilde{v}(t+\tau)] \\ &= \sum_{i, j \in \mathcal{I}} \mathbb{E}[\eta_i(t)\eta_j(t+\tau)] \\ &= \sum_{i, j \in \mathcal{I}} R_{\eta_i \eta_j}(\tau). \end{aligned} \quad (25)$$

The speed perturbation of the truck \tilde{v} as well as its derivative $\dot{\tilde{v}}$ are WSS Gaussian processes with zero mean. Let us consider the second moments

$$\zeta^2 = R_{\tilde{v} \tilde{v}}(0), \quad \vartheta^2 = R_{\dot{\tilde{v}} \dot{\tilde{v}}}(0). \quad (26)$$

Since $R_{\dot{\tilde{v}} \dot{\tilde{v}}}(\tau) = -\frac{d^2}{d\tau^2} R_{\tilde{v} \tilde{v}}(\tau)$, we have

$$\begin{aligned} \vartheta^2 &= -\left. \frac{d^2}{d\tau^2} R_{\tilde{v} \tilde{v}}(\tau) \right|_{\tau=0} \\ &= \mathcal{F}^{-1}[\omega^2 S_{\tilde{v} \tilde{v}}(\omega)] \Big|_{\tau=0} \\ &= \frac{1}{2\pi} \int_{-\infty}^{\infty} \omega^2 S_{\tilde{v} \tilde{v}}(\omega) e^{j\omega\tau} d\omega \Big|_{\tau=0}. \end{aligned} \quad (27)$$

Since $S_{\tilde{v} \tilde{v}}(\omega) = S_{\tilde{v} \tilde{v}}(-\omega)$, we have

$$\vartheta^2 = \frac{1}{\pi} \int_0^{\infty} \omega^2 S_{\tilde{v} \tilde{v}}(\omega) d\omega. \quad (28)$$

Thus, considering $R_{\tilde{v} \dot{\tilde{v}}}(0) = 0$, we can write down the joint distribution of $v = \tilde{v} + v^*$ and $\dot{v} = \dot{\tilde{v}}$ as follows

$$p(v, \dot{v}) = \frac{1}{2\pi\zeta\vartheta} \exp\left(-\frac{(v - v^*)^2}{2\zeta^2} - \frac{\dot{v}^2}{2\vartheta^2}\right). \quad (29)$$

Applying Fubini's theorem, the expected value of the energy consumption w can be calculated as

$$\begin{aligned} \mathbb{E}[w] &= \int_{t_0}^{t_f} dt \int_{-\infty}^{\infty} dv \int_{-\infty}^{\infty} vg(\dot{v})p(v, \dot{v})d\dot{v} \\ &= (t_f - t_0) \int_{-\infty}^{\infty} dv \int_0^{\infty} v\dot{v}p(v, \dot{v})d\dot{v} \\ &= (t_f - t_0) \frac{1}{2\pi\zeta\vartheta} \left[\int_{-\infty}^{\infty} v \exp\left(-\frac{(v - v^*)^2}{2\zeta^2}\right) dv \right] \\ &\quad \times \left[\int_0^{\infty} \dot{v} \exp\left(-\frac{\dot{v}^2}{2\vartheta^2}\right) d\dot{v} \right] \\ &= (t_f - t_0) \frac{v^*}{\sqrt{2\pi}} \vartheta. \end{aligned} \quad (30)$$

That is, the expected value of the energy consumption proportional to ϑ , the standard deviation of \dot{v} . This motivates us to formalize the optimization problem as

$$\begin{aligned} \min (\mathbb{E}[w])^2 &= (t_f - t_0)^2 \frac{(v^*)^2}{2\pi} \vartheta^2 \\ &\propto \int_0^{\infty} \omega^2 S_{\tilde{v} \tilde{v}}(\omega) d\omega \\ &= \sum_{i, j \in \mathcal{I}} \int_0^{\infty} \omega^2 T_i(j\omega)T_j^*(j\omega)S_{\tilde{v}_i \tilde{v}_j}(\omega) d\omega \\ &:= J, \end{aligned} \quad (31)$$

$$\text{such that } (\alpha, \beta_i)_{i \in \mathcal{I}} \in \Omega \quad (32)$$

where Ω is given in (13) and we substituted (28). In the rest of the paper we will use J as a cost function.

B. Data-driven optimization

In practice, we do not know the real value of cross power spectral density of preceding vehicles' speed. Instead, we need to estimate them from data sampled in discrete time with finite length. Such estimation problem has been extensively investigated in literature. Here we utilize two classical methods: periodogram and Welch's method [17].

Given observation data of signal $\{v_i(t_k)\}_{k=0}^{N-1}$ for time instances $t_k = k\Delta t$. First we subtract the sample means to get the centralized data $\{\tilde{v}_i(t_k)\}_{k=0}^{N-1}$. Let $\{\tilde{V}_i(\omega_k)\}_{k=0}^{N-1}$, $\omega_k = \frac{2\pi k}{N\Delta t}$ be the discrete time Fourier transform of $\{\tilde{v}_i(t_k)\}_{k=0}^{N-1}$. Then the periodogram estimator is defined as

$$\hat{S}_{\tilde{v}_i \tilde{v}_i}(\omega_k) = \frac{2\Delta t}{N} |\tilde{V}_i(\omega_k)|^2. \quad (33)$$

The periodogram is fairly good estimator because it is asymptotically unbiased, however, it suffers from high variance. We can alleviate the latter problem using Welch's method [18]. In time domain, we split the original signal into segments with 50% overlap ratio. Then in frequency domain, we apply window function to each segment, e.g., Hamming window, and calculate the periodogram for windowed signals. Finally we average the results for each frequency.

For cross-spectral density estimation, periodogram and Welch's method are similarly defined. Given two signals $\{v_i(t_k)\}_{k=0}^{N-1}$ and $\{v_j(t_k)\}_{k=0}^{N-1}$, and let $\{\tilde{V}_i(\omega_k)\}_{k=0}^{N-1}$ and $\{\tilde{V}_j(\omega_k)\}_{k=0}^{N-1}$ be the discrete time Fourier transform of centralized data $\{\tilde{v}_i(t_k)\}_{k=0}^{N-1}$ and $\{\tilde{v}_j(t_k)\}_{k=0}^{N-1}$, the periodogram method estimates the cross-spectral density with

$$\hat{S}_{\tilde{v}_i \tilde{v}_j}(\omega_k) = \frac{2\Delta t}{N} \tilde{V}_i(\omega_k) \tilde{V}_j^*(\omega_k). \quad (34)$$

Indeed, when $i = j$ this reduces to (33).

It is straightforward to replace the power spectral density $S_{\tilde{v}_i \tilde{v}_j}$ in (31) with periodogram estimator, and rewrite the optimization problem for discrete time observations:

$$\min J \approx \frac{2\Delta t}{N} \sum_{i,j \in \mathcal{I}} \sum_{k=0}^{N-1} \omega_k^2 T_i(j\omega_k) T_j^*(j\omega_k) \tilde{V}_i(\omega_k) \tilde{V}_j^*(\omega_k). \quad (35)$$

The optimization problem is similar for Welch's method. We only need to substitute the cross power spectral density $S_{\tilde{v}_i \tilde{v}_j}(\omega)$ in (31) with estimation results from Welch's method. Notice that we do not need to know the equilibrium velocity v^* in our data-driven method.

We also note that in our previous paper [8] we formalized an optimization problem to determine the energy-optimal controller parameters by minimizing $\sum_{k=1}^{N-1} \omega_k^2 |\tilde{V}(\omega_k)|^2$, which is identical to our optimization problem (35) if we choose the periodogram as spectral estimator. Nevertheless the method presented here gives a new interpretation to this cost function and provides a new method to improve it by choosing a better spectral estimator, e.g. Welch's method.

V. NUMERICAL RESULTS

In this section, we evaluate the optimization method proposed in the previous section using synthetic data. Since the system is stochastic and the parameters are optimized for the average energy consumption, we perform a large amount of simulations and evaluate our algorithm with the statistics of energy consumption. The evaluation scenarios include adaptive cruise control and connected cruise control with a connected vehicle ahead in the traffic.

A. Adaptive cruise control (ACC)

When using ACC, the truck only responds to the vehicle right in front. Therefore the controller (5) simplifies to

$$a_d = \alpha(V(h) - v) + \beta(W(v_1) - v), \quad (36)$$

where we dropped the subscript in β . Correspondingly, the transfer function (11,12) becomes

$$T_1(s) = \frac{\beta s + \alpha \kappa}{s^2 e^{s\sigma} + (\alpha + \beta)s + \alpha \kappa}. \quad (37)$$

We search for the parameter β that minimizes the energy consumption.

The evaluation of our proposed method consists of two steps: observation and testing. In the observation step, we observe the speed profile of the preceding vehicle, estimate the spectral density, and solve the optimization problem (31) to get the optimal gain parameter. In the testing step, we

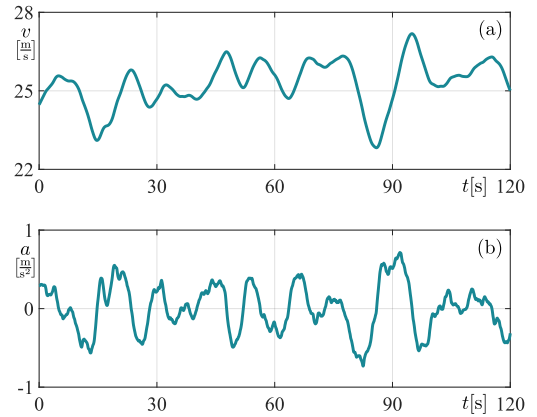


Fig. 2. Sample trajectory of a preceding vehicle. (a) Speed profile. (b) Acceleration profile.

simulate the truck for different preceding vehicle speed profiles using the gain parameter calculated in the observation step. The speed profile of the preceding vehicle in the testing step is generated from the same distribution as in observation step. In particular, we create 101 candidate speed profiles for the preceding vehicle and arbitrarily pick one for observation and another one for testing.

The candidate speed profiles are independently generated from Gaussian process with Matérn kernel

$$R_{\tilde{v}_1 \tilde{v}_1}(\tau) = C^2 \frac{2^{1-\nu}}{\Gamma(\nu)} \left(\sqrt{2\nu} \frac{\tau}{\rho} \right)^\nu K_\nu \left(\sqrt{2\nu} \frac{\tau}{\rho} \right), \quad (38)$$

where $\Gamma(\cdot)$ is the Gamma function, $K_\nu(\cdot)$ is the modified Bessel function of the second kind, and ρ and ν are positive parameters. In our simulations, we choose $v^* = 25$ [m/s], $C = 1$, $\rho = 5$, and $\nu = \frac{5}{2}$. It can be proved that this process is second-order mean square differentiable [19]. A sample speed profile and the corresponding acceleration profile are plotted in Fig. 2(a) and (b) respectively. Each candidate speed profile has 2 minute duration.

Fig. 3 plots statistics of the 101 candidate speed profiles in time domain and frequency domain. In time domain, we calculate sample autocorrelation for each candidate trajectory and plot the mean (cyan solid curve) and the standard deviation (cyan shading) in Fig. 3(a). We also plot function (38) as purple dashed curve for comparison that we refer to as the "oracle". Observe that the mean of sample autocorrelation function matches the oracle very well. In frequency domain, we calculate the power spectral density using the periodogram (orange curve and shading) and Welch's method (green curve and shading) and compare them with the oracle power spectral density (purple dashed curve) in Fig. 3(b). The latter one is obtained as the Fourier transform of (38). The mean of spectral estimators matches the oracle very well except at zero frequency. Note that the spectral density at zero frequency does not influence the objective function (31). The periodogram estimator has higher resolution compared to Welch's method, but the variance is significantly higher.

In order to show the optimality of our proposed method, we first apply grid search to find the "ground truth" optimal parameter. For each candidate trajectory, we simulate the

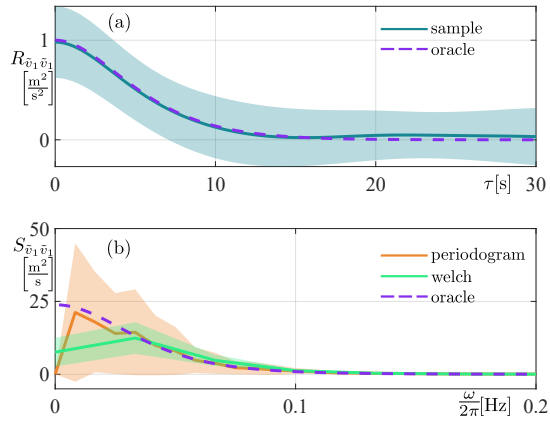


Fig. 3. Statistics of 101 candidate speed profiles. (a) Sample correlation function and the oracle correlation function (38). (b) Spectral estimations according to the 101 candidate speed profiles and the oracle power spectral density. Solid curves denote the mean while the standard deviation is indicated by shading.

truck using different β values between 0 and 1 [1/s] with step size 0.01 [1/s] while fixing $\alpha = 0.4$ [1/s]. The initial condition is set to be $v(t) \equiv v^*$, $h(t) \equiv h^*$ for $t \in [-\sigma, 0]$. We conduct simulations using the nonlinear model (1,4,5) as well as the linear model (9) and plot the statistics of the energy consumption in Fig. 4, where solid curves indicate the mean and shadings indicate the standard deviation. The optimal parameters, which results in minimum average energy consumption, are marked by crosses in both cases. They are located at $\beta_{\text{lin}}^* = 0.54$ [1/s] and $\beta_{\text{nonlin}}^* = 0.63$ [1/s] for linear and nonlinear simulations, respectively. For comparison, we also plot the cost function J which is calculated with oracle knowledge of spectral density. The shape of this curve is similar to the curve of average energy consumption in Fig. 4(a) and it reaches its minimum at $\beta_o = 0.58$ [1/s].

Considering the 101 candidate speed profiles, there are $101 \times 100 = 10100$ observation-testing pairs available to evaluate our optimization method. In the observation step, the spectral density may come from the spectral estimators (periodogram or Welch's method), or potentially from oracle knowledge. These spectral densities are then plugged into (31), and the resulting optimal parameters are denoted as β_p , β_w , and β_o . We use these optimized parameters in the testing step and denote the corresponding energy consumption values as w_p , w_w , and w_o , respectively. For each testing trajectory, since we have simulated for all β ranging between 0 and 1 [1/s], we know the ground truth of the energy-optimal parameter and the corresponding minimum energy consumption w^* . The sub-optimality of β_p , β_w and β_o can be evaluated using the differences $\Delta w_p = w_p - w^*$, $\Delta w_w = w_w - w^*$ and $\Delta w_o = w_o - w^*$.

We visualize these differences for all 10100 observation-testing pairs using the histograms in Fig. 5(a) and (b) for the linear and nonlinear simulations, respectively. In general, Δw_p , Δw_w and Δw_o are all concentrated around 0, which means with high probability, the energy consumption w_p , w_w and w_o are all very close to the optimal value w^* . Notice, however, that Δw_o has lighter tails than Δw_p and Δw_w , so

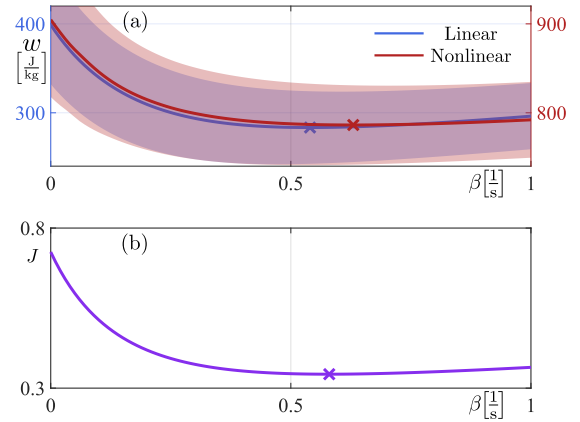


Fig. 4. (a) Energy consumption obtained by simulating the linear (blue) and the nonlinear (red) truck models. Solid curves denote the mean, the standard deviation is indicated by shading, and crosses mark the gain parameters β_{lin}^* and β_{nonlin}^* with minimum average energy consumption. (b) Cost function J with oracle knowledge of spectral density with a cross marking β_o .

the parameters chosen from the oracle spectral density are closer to the ground truth optimal. Since in general we do not have access to the oracle knowledge of spectral density, it is important to compare the two estimation methods. The histograms in Fig. 5(c) and (d) depict $\Delta w_{\text{pw}} = w_p - w_w$ for the linear and nonlinear simulation, respectively. Among all 10100 observation-testing pairs, Welch's method consumes less energy than periodogram method in 56% cases for linear simulations and in 61% cases for nonlinear simulations. So in ACC scenario, Welch's method outperforms periodogram.

B. Connected cruise control (CCC)

When implementing CCC we assume that the truck responds to vehicle 1 immediately ahead as well as to vehicle L further ahead, which is connected to the truck through V2V communication; see Fig. 1(a). This so-called leading vehicle is not necessarily adjacent to vehicle 1. Since the speed of leading vehicle L can influence the speed of vehicle 1, we generate speed trajectories for vehicle L with Gaussian process described in (38), and then simulate the vehicle chain from vehicle 1 to L using the human driver model

$$\dot{v}_i(t) = \alpha_h (V_h(h_i(t - \sigma_h)) - v_i(t - \sigma_h)) + \beta_h (W(v_{i+1}(t - \sigma_h)) - v_i(t - \sigma_h)), \quad (39)$$

for $i = 1, \dots, L - 1$. We use the nonlinear range policy

$$V_h(h) = \max \{0, \min \{ \kappa_h (h - h_{\text{st}}), v_{\text{max}} \} \}, \quad (40)$$

(cf. (6)) and the speed policy W is defined in (7). We use $L = 8$, $\alpha_h = 0.1$ [1/s], $\beta_h = 0.4$ [1/s], $\kappa_h = 1.0$ [1/s] and $\sigma_h = 1.0$ [s]. Similar to the ACC case, we generate 101 candidate speed profiles for vehicles L and 1, and evaluate our proposed methods for all observation-testing pairs.

Again we fix $\alpha = 0.4$ [1/s] and optimize for the parameters β_1 and β_L . We search for all $(\beta, \beta_L) \in [0, 1] \times [0, 1]$ [1/s] with step size 0.05 [1/s] to find the ground truth for each candidate speed profile. For the 10100 observation-testing pairs, we evaluate w_p , w_w , and w_o and compare them to the ground-truth energy consumption w^* . In Fig. 6(a) and

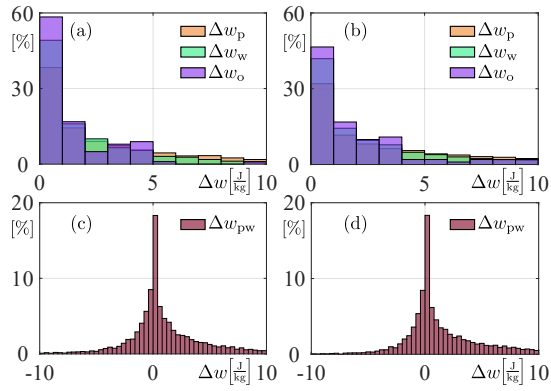


Fig. 5. Histogram of Δw_p , Δw_w , Δw_o and w_{pw} for ACC. Panels (a), (c) show linear simulation results while (b), (d) show nonlinear results.

(b) we plot the histogram of Δw_p , Δw_w and Δw_o for linear and nonlinear simulations, respectively. In both cases, the histograms are concentrated around zero. In this case, Welch’s method is even more advantageous compared to oracle’s method and periodogram method. Still, the oracle method is better than the periodogram. In Fig. 6(c) and (d) we directly compare the periodogram and Welch’s method and show that Welch’s method consumes less energy than periodogram for 65% cases in linear simulations, and for 65% cases in nonlinear simulations. Therefore in case of CCC, Welch’s method still outperforms the periodogram.

VI. CONCLUSION

A class of longitudinal controllers was investigated for a connected automated truck traveling in a mixed traffic consisting of connected and non-connected human-driven vehicles. The proposed connected cruise controller utilized information about the position and velocity of preceding vehicles from on-board sensors and V2V communication and it was applicable for lean penetration of automation and connectivity. In order to determine the energy-optimal controller parameters, we modeled the speed of preceding vehicles as wide-sense stationary, mean-square differentiable Gaussian processes, and formalized an optimization problem that minimized the average energy consumption using spectral analysis and spectral estimation. The optimality of our method was validated statistically with large number of simulations. We also showed that choosing better spectral estimator can improve the energy efficiency. Generalization to broader class of stochastic processes is left for future work.

REFERENCES

- [1] A. Vahidi and A. Sciarretta, “Energy saving potentials of connected and automated vehicles,” *Transportation Research Part C*, vol. 95, pp. 822–843, 2018.
- [2] B. McAuliffe, M. Lammert, X.-Y. Lu, S. Shladover, M.-D. Surcel, and A. Kailas, “Influences on energy savings of heavy trucks using cooperative adaptive cruise control,” in *WCX World Congress Experience*. SAE International, 2018.
- [3] L. Bertoni, J. Guanetti, M. Basso, M. Masoero, S. Cetinkunt, and F. Borrelli, “An adaptive cruise control for connected energy-saving electric vehicles,” *IFAC-PapersOnLine*, vol. 50, no. 1, pp. 2359–2364, 2017, 20th IFAC World Congress.
- [4] K. Liang, J. Mårtensson, and K. H. Johansson, “Heavy-duty vehicle platoon formation for fuel efficiency,” *IEEE Transactions on Intelligent Transportation Systems*, vol. 17, no. 4, pp. 1051–1061, 2016.

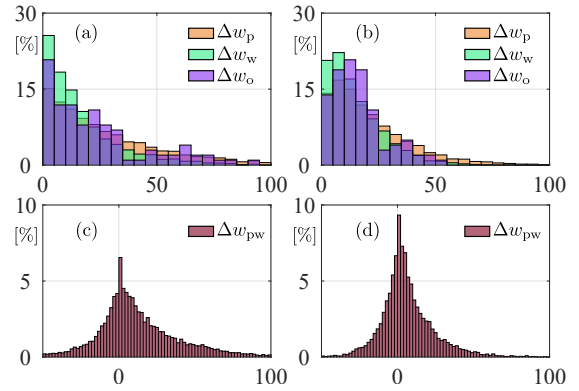


Fig. 6. Histogram of Δw_p , Δw_w , Δw_o and w_{pw} for CCC. Panels (a), (c) show linear simulation results while (b), (d) show nonlinear results.

- [5] L. Zhang, F. Chen, X. Ma, and X. Pan, “Fuel economy in truck platooning: a literature overview and directions for future research,” *Journal of Advanced Transportation*, vol. 2020, 2020.
- [6] L. Zhang and G. Orosz, “Motif-based design for connected vehicle systems in presence of heterogeneous connectivity structures and time delays,” *IEEE Transactions on Intelligent Transportation Systems*, vol. 17, no. 6, pp. 1638–1651, 2016.
- [7] G. Orosz, “Connected cruise control: modelling, delay effects, and nonlinear behaviour,” *Vehicle System Dynamics*, vol. 54, no. 8, pp. 1147–1176, 2016.
- [8] C. R. He, J. I. Ge, and G. Orosz, “Fuel efficient connected cruise control for heavy-duty trucks in real traffic,” *IEEE Transactions on Control Systems Technology*, vol. 28, no. 6, pp. 2474–2481, 2020.
- [9] G. Orosz, J. I. Ge, C. R. He, S. S. Avedisov, W. B. Qin, and L. Zhang, “Seeing beyond the line of site – controlling connected automated vehicles,” *ASME Mechanical Engineering Magazine*, vol. 139, no. 12, pp. S8–S12, 2017.
- [10] J. Jing, A. Kurt, E. Ozatay, J. Michelini, D. Filev, and U. Ozguner, “Vehicle speed prediction in a convoy using V2V communication,” in *2015 IEEE 18th International Conference on Intelligent Transportation Systems*, 2015, pp. 2861–2868.
- [11] L. Zhang and E. Tseng, “Motion prediction of human-driven vehicles in mixed traffic with connected autonomous vehicles,” in *2020 American Control Conference (ACC)*. IEEE, 2020, pp. 398–403.
- [12] S. Wong, L. Jiang, R. Walters, T. G. Molnár, G. Orosz, and R. Yu, “Traffic forecasting using vehicle-to-vehicle communication,” in *Learning for Dynamics and Control*. PMLR, 2021, pp. 917–929.
- [13] C. Huang, R. Salehi, T. Ersal, and A. G. Stefanopoulou, “An energy and emission conscious adaptive cruise controller for a connected automated diesel truck,” *Vehicle System Dynamics*, vol. 58, no. 5, pp. 805–825, 2020.
- [14] S. V. D. Hoef, J. Mårtensson, D. V. Dimarogonas, and K. H. Johansson, “A predictive framework for dynamic heavy-duty vehicle platoon coordination,” *ACM Transactions on Cyber-Physical Systems*, vol. 4, no. 1, 2019.
- [15] J. I. Ge, S. S. Avedisov, C. R. He, W. B. Qin, M. Sadeghpour, and G. Orosz, “Experimental validation of connected automated vehicle design among human-driven vehicles,” *Transportation Research Part C*, vol. 91, pp. 335–352, 2018.
- [16] B. Hajek, *Random processes for engineers*. Cambridge University Press, 2015.
- [17] R. H. Shumway and D. S. Stoffer, *Time Series Analysis and Its Applications*. Springer, 2000.
- [18] P. Welch, “The use of fast Fourier transform for the estimation of power spectra: A method based on time averaging over short, modified periodograms,” *IEEE Transactions on Audio and Electroacoustics*, vol. 15, no. 2, pp. 70–73, 1967.
- [19] C. Rasmussen and C. Williams, *Gaussian Processes for Machine Learning*. MIT Press, 2006.